Transient Diffusion from a Well-Stirred Reservoir to a Body of Arbitrary Shape

YI HUA MA and LAWRENCE B. EVANS
Massachusetts Institute of Technology, Cambridge, Massachusetts

A theoretical study was made of transient diffusion to a body immersed in a finite volume of well-stirred fluid. The major contribution of this work was the development of a technique for solving the problem for a three-dimensional body of arbitrary shape. The solutions are in a form that is useful for determining diffusion coefficients in solids by means of the constant-volume experimental technique.

The partial differential equation coupled with the ordinary differential equation describing the diffusion process is transformed into a single integral equation in terms of the solute concentration in the reservoir. A numerical technique is then presented for solving the integral equation. Numerical solutions were computed for the three geometries that possess analytical solutions: the infinite slab, the infinite cylinder, and the sphere. By properly choosing the step-size numerical results were easily obtained that agreed with the exact solution to four decimal places.

New solutions were computed for two three-dimensional geometries: the finite cylinder and the rectangular prism. A range of shape factors and ratios of the volume of the reservoir to that of the solid body were employed for each geometry. It was shown that by selecting the ratio of volume to external surface area as the characteristic length of each shape object, the solutions for all shapes were brought close together and were identical during the initial part of the transient.

Previously reported solutions to the problem of transient diffusion to a solid object immersed in a finite volume of well-stirred fluid as summarized by Crank (*2*) have been restricted to the simple one-dimensional shapes of an infinite slab, an infinite circular cylinder, and a sphere. In the work reported herein a technique was developed to allow for arbitrary shapes.

Diffusive transfer of heat or mass between a solid and a limited quantity of fluid is an important phenomena in such diverse applications as dying of films and fibers, quenching of hot solids, solid-liquid extraction, and batch chemical reaction in a porous catalyst. It is also the basis for the constant-volume technique of determining diffusion coefficients in solids by experimentally measuring the rate of depletion of solute from a fixed quantity of fluid, during sorption by the solid phase. March and Weaver (*6*) employed this technique to measure rates of diffusion of urea from solution into a gel; Wagner (*8*) applied the method to investigate diffusion by isotopic exchange between solid and gas; Wilson (*9*) and Crank (*3, 4*) studied the rate of diffusion of dye from a dyebath into a film; and, Carman and Haul (*1*) showed that the method gave satisfactory results for the rate of adsorption of both butane and argon on a single Linde silica plug.

In order to use the constant-volume method, one must have theoretical solutions that are valid for the particular shape of particle used in the experiments. The diffusion coefficient can then be determined to force the experimental data to fit the theoretical solution. Use of the technique has been handicapped heretofore by the lack of solutions for three-dimensional shapes. Questions have frequently arisen as to whether unusual experimental behavior was due to edge effects or was the result of unexpected phenomena such as temperature effects, adsorption, or chemical reaction. The results of this work should help in resolving some of these questions.

To simplify the discussion, the problem will be presented in terms of the diffusion of a single solute in a homogeneous solid phase. The results are directly applicable, however, to heat conduction, to diffusion in a porous solid, and to permeation of pure gases and liquids in a solid matrix, since all of these systems obey the same governing equations in a dimensionless form. The results may also be applied to the problem of diffusion with rapid adsorption, if the adsorption isotherm is linear, by using the transformation discussed by Wilson (*11*).

MATHEMATICAL DERIVATIONS

Mathematical Model

Consider a solid of arbitrary shape and volume, V_S, immersed in a reservoir of well-stirred fluid of volume, V_F. The concentration, $c(\vec{r}, t)$, of solute in the solid and the

Yi Hua Ma is with the Worcester Polytechnic Institute, Worcester, Massachusetts.

concentration, $y(t)$, of solute in the fluid are described by the linear differential equations

$$\nabla^2 c = \frac{1}{D} \frac{\partial c}{\partial t} \tag{1}$$

$$V_F \frac{dy}{dt} = - \oiint D \, \vec{\nabla} c \cdot d\vec{S} \tag{2}$$

with the boundary conditions:

for $t = 0$, within the fluid: $y = y_i$ (3a)

for $t = 0$, throughout the solid: $c = c_i$ (3b)

for $t > 0$, at the solid boundary: $c = y$ (3c)

where D, the effective diffusivity of solute in the solid, is constant. These boundary conditions assume that the solute distribution in the solid is initially uniform and that there is no mass transfer resistance at the solid-fluid interface.

Equation (2), which equates the rate of solute accumulation in the fluid to the net rate of diffusion across the boundary, can be transformed by means of the divergence theorem to the equivalent form:

$$V_F \frac{dy}{dt} = - \int_{V_S} \frac{\partial c}{\partial t} \, dV \tag{4}$$

If one defines the following dimensionless quantities: $C = (c - c_i)/(y_i - c_i)$, $Y = (y - c_i)/(y_i - c_i)$, $\theta = Dt/L^2$, and $\vec{R} = \vec{r}/L$, where L is some characteristic length of the solid, then Equations (1) and (4) become

$$\nabla^2 C = \frac{\partial C}{\partial \theta} \tag{5}$$

$$V_F \frac{dY}{d\theta} = - \int_{V_S} \frac{\partial C}{\partial \theta} \, dV \tag{6}$$

with the dimensionless boundary conditions:

for $\theta = 0$, within the fluid: $Y = 1$ (7a)

for $\theta = 0$, throughout the solid: $C = 0$ (7b)

for $\theta > 0$, at the solid boundary: $C = Y$ (7c)

The analytical solutions to the above equations, as summarized by Crank (2), for the one-dimensional slab, the infinite circular cylinder, and the sphere, give both the concentration $C(\vec{R}, \theta)$ within the solid, as a function of position and time, and the concentration $Y(\theta)$ in the fluid as a function of time. In most practical applications, $Y(\theta)$, or the net rate of transfer, is all that is of interest.

Transformation to an Integral Equation

In the derivation which follows, the problem of solving Equations (5), (6), and (7) will be reduced to the less difficult problem of solving a single integral equation for $Y(\theta)$. The method requires only that a solution be available to the problem of transient diffusion in the solid alone as described by Equation (5) with the boundary conditions:

for $\theta = 0$, within the solid: $C = 0$ (8a)

for $\theta > 0$, at the solid boundary: $C = 1$ (8b)

Let $F(\vec{R}, \theta)$ denote the solution to this problem.

Now, the dimensionless concentration of solute in the solid following imposition of an arbitrary time-varying surface concentration $Y(\theta)$, that is, with the boundary condition (8b) replaced by

for $\theta > 0$, at the solid boundary: $C = Y(\theta)$ (9)

is given by the Duhamel integral:

$$C = C(\vec{R}, \theta) = F(\vec{R}, \theta) Y(\theta = 0) + \int_0^\theta Y'(\xi) F(\vec{R}, \theta - \xi) \, d\xi \tag{10}$$

where $Y'(\xi)$ is used to denote $dY/d\xi$.

Integrating Equation (6) gives:

$$V_F(Y(\theta) - 1) = - \int_{V_S} C dV \tag{11}$$

Dividing each term in Equation (11) by V_S and rearranging yields:

$$\alpha \, Y(\theta) + \frac{1}{V_S} \int_{V_S} C dV = \alpha \tag{12}$$

where

$$\alpha = \frac{V_F}{V_S} = \frac{\text{volume of fluid}}{\text{volume of solid}} \tag{13}$$

By substituting Equation (10) into Equation (12) we obtain

$$\alpha \, Y(\theta) + \frac{1}{V_S} \int F(\vec{R}, \theta) \, dV + \frac{1}{V_S} \int \int_0^\theta Y'(\xi) F(\vec{R}, \theta - \xi) \, d\xi dV = \alpha \tag{14}$$

Now, we denote

$$f(\theta) = \frac{1}{V_S} \int_{V_S} F(\vec{R}, \theta) \, dV \tag{15}$$

and (14) can be rewritten as

$$\alpha \, Y(\theta) + f(\theta) + \int_0^\theta Y'(\xi) \, f(\theta - \xi) \, d\xi = \alpha \tag{16}$$

This is an integral equation whose solution $Y(\theta)$ gives the solute concentration in the fluid as a function of time. The problem has thus been reduced from that of solving a partial differential equation coupled with an ordinary differential equation to one of solving an integral equation. A similar approach was used by March and Weaver (6) to derive their analytical solution for an infinite slab.

The function $f(\theta)$ is the dimensionless, volume-average solute concentration in the solid for the case of a constant surface concentration. It will depend only upon the particular shape and the characteristic length chosen in defining θ. Examples of $f(\theta)$ for an infinite slab, an infinite cylinder, a rectangular prism, and a sphere are shown in Appendix A. The characteristic length and shape factor for each geometry considered in this work are shown in Figure 1.

Method of Presenting Solutions

In the limit as θ approaches infinity, $C(\theta)$ and $Y(\theta)$

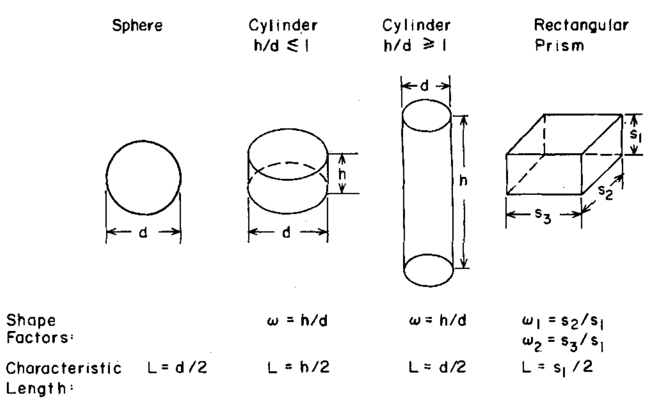

Fig. 1. Dimensions, shape factors, and characteristic length for each geometry.

both approach the same limiting values:

$$C_\infty = Y_\infty = \frac{\alpha}{1 + \alpha} \tag{17}$$

A form of solution, which is convenient for comparison with experimental measurements, is the relation between M_t/M_∞ and time, where M_t and M_∞ are the net change in solute in the solid at time t and time infinity, respectively.

$$\frac{M_t}{M_\infty} = \frac{y_i - y(t)}{y_i - y_\infty} \tag{18}$$

This can also be interpreted as the fractional approach of the solute concentration to its steady state value. In terms of the dimensionless variables,

$$\frac{M_t}{M_\infty} = (1 + \alpha)\,[1 - Y(\theta)] \tag{19}$$

It is also convenient to express α in terms of the ratio

$$\epsilon \equiv \frac{1}{1 + \alpha} \tag{20}$$

which is the fraction of total volume that is occupied by solid. Crank (2) calls this the *final fractional uptake,* because for the case of $c_i = 0$ it is the fraction of total solute initially present in the liquid that is finally taken up by the solid. The case of $\epsilon = 0$ or $\alpha = \infty$ corresponds to an infinite reservoir in which the fluid concentration does not change. For this case $Y(\theta) \equiv 1$ and $M_t/M_\infty = f(\theta)$.

NUMERICAL METHOD

As can be seen from the examples in Appendix A, the form of $f(\theta)$ will generally be so complicated that analytical solution of Equation (16) is not practical and solutions must be obtained numerically. A variety of methods have been proposed; most of them are discussed by Noble (7) in his review. All of the methods are based upon representing the known function, $f(\theta)$, and the unknown functions, $Y(\theta)$ and $Y'(\theta)$, in terms of a set of values, $f_n = f(\theta_n)$ and $Y_n = Y(\theta_n)$, where θ_n $(n = 0, 1 \ldots)$ is a set of discrete values of the ordinate θ. It is common to use equally spaced ordinates for which $\theta_n = n\Delta\theta$, where $\Delta\theta$ is the step size. The various numerical methods that have been proposed differ in the technique used to solve for the unknown set of values Y_n such that they approximate the true solution to the integral equation. The numerical solutions obtained in this work were computed by using a slight modification of a method proposed by Laudet and Oulès (5). The method is summarized in Appendix B.

To test the numerical method, solutions were computed for three geometries possessing analytical solutions: the infinite slab, the infinite cylinder, and the sphere. The effect of the step size is shown in Table 1 in which values of M_t/M_∞ are tabulated for an infinite slab with • = 0.5. The exact analytical solution is tabulated along with values for different step sizes. It can be seen that for a step size $\Delta\theta = 0.001$, the numerical solution agreed to four decimal places with the exact solution except at very small values of θ. The accuracy of the solutions for all step sizes improves as θ increases. Equally satisfactory results were achieved for the other geometries and for all values of ϵ. About 20 sec. of computing time on the IBM 7094 was required to compute the solution in Table 1 for $\Delta\theta = 0.001$.

TABLE 1. VALUES OF M_t/M_∞ COMPUTED FOR AN INFINITE SLAB WITH $\epsilon = 0.50$

	Numerical Solutions			Exact
θ	$\Delta\theta = 0.10$	$\Delta\theta = 0.01$	$\Delta\theta = 0.001$	Solution
0.005	—	—	0.150308	0.150085
0.20	0.7475	0.7122	0.711645	0.711646
0.50	0.9234	0.9166	0.916471	0.916476

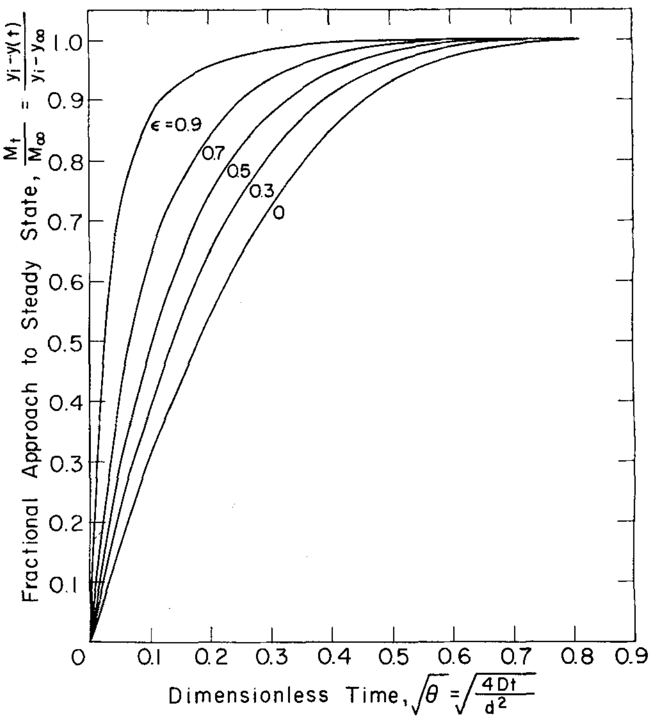

Fig. 2. Approach to steady state for a cylinder with height equal to diameter ($\omega = 1$).

SOLUTIONS FOR THREE-DIMENSIONAL BODIES

Numerical solutions to Equation (16) were obtained for thirteen three-dimensional shapes. The shapes included finite cylinders with ratios of height to diameter, ω = 0.0625, 0.25, 0.50, 1.0, 2.0, 4.0, and 16, and rectangular prisms with combinations of ratios of the two longest sides to the shortest side equal to (1, 1), (1, 16), (2, 2), (16, 16), (1, 2), and (2, 16). Tabulations of M_t/M_∞ are presented in Appendix C* for θ = 0.0001 (0.0001) 0.001 (0.001) 0.01 (0.01) 0.10 (0.05) 0.50 and ϵ = 0, 0.3, 0.5, 0.7, and 0.9. The characteristic lengths used in defining θ are shown in Figure 1.

Illustrative plots of M_t/M_∞ are shown in Figure 2 for a circular cylinder with $\omega = 1$ and in Figure 3 for a cube ($\omega_1 = \omega_2 = 1$). These curves show, as expected, that the greater the fraction volume occupied by the solid, the faster the solute is removed from solution. The diffusion coefficient could be determined from experimental data by comparing the experimentally observed rate of fall of concentration in the solution with the corresponding calculated curve showing M_t/M_∞ as a function of dimensionless time.

A much abbreviated table of values of M_t/M_∞ for all the shapes used in the calculations as well as the results for an infinite slab, an infinite cylinder, and a sphere are presented in Table 2. It is interesting to note that for a finite cylinder with $\omega = 16$ the solution presented here approaches that for an infinite cylinder. In fact, for $\omega = 4$, the present solution is within about 10% of the solution for the infinite cylinder, indicating that end effects are not

* Appendix C has been deposited as document NAPS-00139 with the ASIS National Auxiliary Publications Service, c/o CCM Information Sciences, Inc., 212 W. 34 St., N. Y. 10001 and may be obtained for $3.00 for photoprints or $1.00 for 35mm. microfilm.

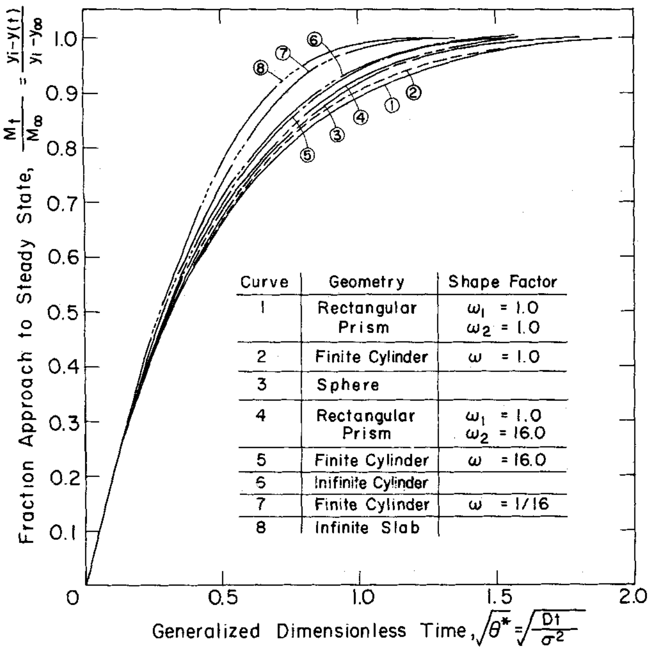

Fig. 3. Approach to steady state for a cube ($\omega_1 = \omega_2 = 1$).

great, even for a cylindrical shape whose height is only four times its diameter. The solution for $\omega = 1/16$ approaches the solution for a one-dimensional slab. Clearly, this is to be expected as the value of ω becomes small. The solutions for the cube are close to those for a sphere, particularly at low values of final fractional uptake. For the rectangular prism with $\omega_1 = \omega_2 = 16$, the results are very close to those for the infinite slab.

In an effort to obtain a correlation for use with any arbitrary shape, M_t/M_∞ was plotted versus a generalized dimensionless time, $\theta^* = Dt/\sigma^2$, where σ is the ratio of the volume of the solid to its external surface area. The results are shown in Figures 4 and 5 for values of ϵ equal to 0 and 0.5, respectively. It can be seen from these figures that the curves corresponding to different shapes are brought close together with this type of plot. The spread between curves for different shapes decreases as the fraction of volume occupied by the solid increases. At small time, all the

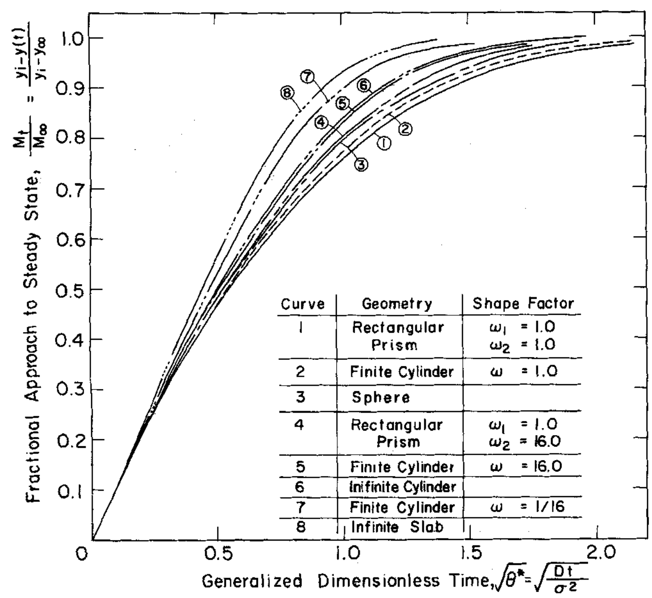

Fig. 4. Approach to steady state for $\epsilon = 0$ with dimensionless time based on volume-to-surface ratio.

TABLE 2. NUMERICAL VALUES OF M_t/M_∞ FOR ALL GEOMETRIES STUDIED

		Finite Cylinder							Infinite		Rectangular Prism						Infinite
ϵ	θ	$\omega=1/16$	$\omega=1/4$	$\omega=1/2$	$\omega=1$	$\omega=2$	$\omega=4$	$\omega=16$	Cylinder	Sphere	$\omega_1=1$, $\omega_2=1$	$\omega_1=1$, $\omega_2=2$	$\omega_1=1$, $\omega_2=16$	$\omega_1=2$, $\omega_2=16$	$\omega_1=2$, $\omega_2=2$	$\omega_1=16$, $\omega_2=16$	Slab
0	0.01	0.1253	0.1623	0.2107	0.3040	0.2597	0.2376	0.2210	0.2156	0.3048	0.3107	0.2573	0.2185	0.1688	0.2101	0.1253	0.1128
0	0.09	0.3663	0.4467	0.5471	0.7225	0.6515	0.6160	0.5894	0.5805	0.7425	0.7105	0.6365	0.5716	0.4621	0.5435	0.3662	0.3385
0	0.25	0.5927	0.6787	0.7802	0.9286	0.8830	0.8600	0.8428	0.8370	0.9473	0.9161	0.8624	0.8151	0.6968	0.7744	0.5926	0.5622
0	0.50	0.7870	0.8505	0.9200	0.9909	0.9769	0.9692	0.9635	0.9616	0.9955	0.9868	0.9665	0.9471	0.8652	0.9147	0.7869	0.7639
0.50	0.001	0.0775	0.1014	0.1324	0.1913	0.1627	0.1481	0.1370	0.1333	0.2397	0.1908	0.1622	0.1365	0.1054	0.1323	0.0775	0.0694
0.5	0.04	0.4120	0.4945	0.5889	0.7357	0.6754	0.6431	0.6179	0.6091	0.7497	0.7287	0.6666	0.6072	0.5088	0.5865	0.4120	0.3820
0.5	0.15	0.6733	0.7503	0.8316	0.9390	0.9056	0.8882	0.8748	0.8690	0.9529	0.9288	0.8902	0.8553	0.7650	0.8276	0.6732	0.6438
0.5	0.50	0.9274	0.9513	0.9776	0.9988	0.9961	0.9948	0.9941	0.9938	0.9996	0.9978	0.9928	0.9887	0.9578	0.9751	0.9259	0.9165
0.9	0.0001	0.1163	0.1504	0.1931	0.2694	0.2398	0.2135	0.1985	0.1933	0.2600	0.2688	0.2323	0.1981	0.1558	0.1928	0.1163	0.1044
0.9	0.005	0.5305	0.6111	0.7296	0.7925	0.7514	0.7267	0.7059	0.6962	0.8001	0.7890	0.7468	0.7003	0.6230	0.6892	0.5305	0.4978
0.9	0.04	0.8221	0.8678	0.9080	0.9538	0.9379	0.9287	0.9212	0.9179	0.9581	0.9513	0.9341	0.9159	0.8751	0.9068	0.8221	0.8016
0.9	0.50	0.9959	0.9962	0.9982	0.9996	0.9988	0.9948	0.9984	0.9999	1.0000	1.0000	0.9974	0.9963	0.9830	0.9979	0.9711	0.9963

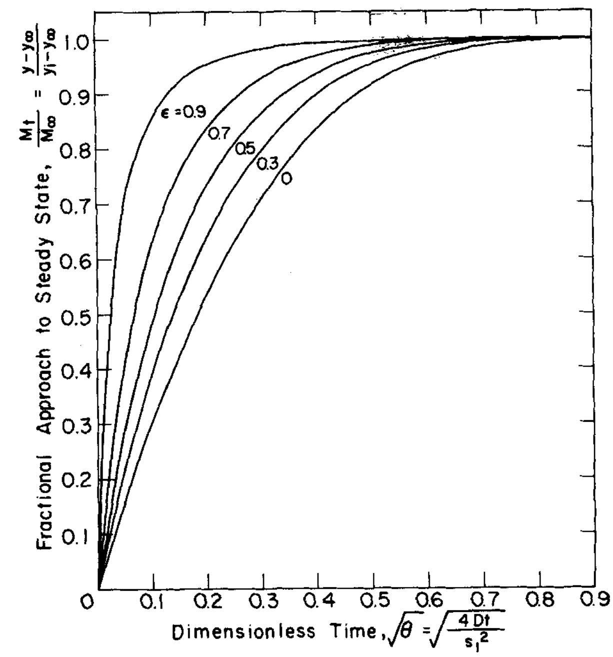

Fig. 5. Approach to steady state for $\epsilon = 0.50$ with dimensionless time based on volume-to-surface ratio.

curves coincide. Physically this can be explained by the fact that at small time when there has been little penetration of solute into the solid, three-dimensional effects are unimportant and the surface area is all that matters.

The diffusion coefficient for a solid with arbitrary shape could be determined by carrying out an experiment for a short period of time and comparing the results with any available theoretical solution for which M_t/M_∞ is plotted vs. θ^*. In order to have an idea of the maximum actual time which still satisfies the notion of short time, consider an arbitrary shape with $\sigma = 1$ cm. From Figures 4 and 5, one sees that the curves for all shapes coincide up to $\theta^* = 0.2$. For a diffusion coefficient of 10^{-5} sq.cm./sec., the actual time could be as long as 4,000 sec., which would provide a sufficient time for accurate experimental measurement of the solute concentration. It can be seen from Figures 4 and 5 that the curves for objects of similar shape tend to lie close together. The solutions for shapes similar to that of a sphere (for example, the cube or cylinder with $\omega = 1$) form the lowest branch of the family of curves; the solution for the infinite slab is the highest branch of the family; and that for the infinite cylinder is in the middle. This suggests that with some caution, an approximate solution for M_t/M_∞ vs. θ^* might be constructed for an arbitrary shape by judiciously interpolating between the curves for similar shapes on a plot such as Figure 4 or 5. It appears that this type of approximation would be valid to within about 10%.

SUMMARY AND CONCLUSIONS

A new approach has been used to treat the problem of transient diffusion to a body immersed in a well-stirred reservoir. It was shown that the partial differential equation coupled with an ordinary differential equation could be reduced to a single integral equation in terms of the solute concentration in the reservoir. All that is required is that a solution for the geometry in question be available to the uncoupled problem of transient diffusion in the solid body alone exposed to a constant surface concentration. This solution need not necessarily be analytical; a numerical solution, or even the results from an experimental analog will do as well, since only tabulated values of the function $f(\theta)$ are required to solve the integral equation numerically. If the complete concentration distribution in the solid is needed, it can be obtained by use of Duhamel's integral as indicated in Equation (10) once the integral equation has been solved for $Y(\theta)$.

It was demonstrated that the numerical method proposed by Laudet and Oulès (5) was satisfactory for solving the integral equation. Numerical solutions were obtained for three geometries possessing analytical solutions: the infinite slab, the infinite cylinder, and the sphere. It was not difficult to compute solutions which agreed with the exact analytical solution to four decimal places.

To illustrate the technique described above, solutions for M_t/M_∞ were computed for two new geometries: the finite cylinder and the rectangular prism. A range of shape factors and values of the final fractional uptake were employed for each geometry. These solutions can be used directly with the constant-volume experimental method to measure diffusion coefficients in solids.

It was shown that by defining a generalized dimensionless time θ^* based on the ratio of volume to external surface area as the characteristic length, the solutions for M_t/M_∞ vs. θ^* for all of the shapes were brought close together. The solutions coincide in fact during the initial part of the transient.

ACKNOWLEDGMENT

Part of this research has been supported by the National Science Foundation. Use of the facilities of the Mass. Inst. Tech. Computation Center is gratefully acknowledged.

NOTATION

- c = concentration of solute within the solid body
- C = dimensionless concentration of solute within solid body, $(c - c_i)/(y_i - c_i)$
- D = diffusion coefficient in the body
- d = diameter of cylinder or sphere
- $\vec{dS}$ = vectorial differential element of surface area
- dV = differential element of volume
- $f(\theta)$ = dimensionless volume-average solute concentration in the solid, defined by Equation (15), for transient diffusion in the solid alone exposed to a constant surface concentration
- $f_c(\theta)$ = $f(\theta)$ for an infinite cylinder, see Equation (A2)
- $f_s(\theta)$ = $f(\theta)$ for an infinite slab, see Equation (A3)
- F = volume-average solute concentration in the solid alone exposed to a constant surface concentration
- h = height of cylinder
- J_o = Bessel function of the first kind
- L = characteristic length of solid body, see Figure 1 for definition applicable to each geometry
- M_t = mass of solute transferred from reservoir to the solid body at time t
- M_∞ = mass of solute transferred from reservoir to the solid body at time infinity
- $\vec{r}$ = vector denoting position within the solid body
- $\vec{R}$ = dimensionless vector denoting position within the solid body
- s_1, s_2, s_3 = length of sides of rectangular prism (s_1 = length of shortest side)
- t = time since the solid body was immersed in the reservoir
- y = solute concentration in the reservoir
- Y = dimensionless solute concentration in the reservoir, $(y - c_i)/(y_i - c_i)$
- Y' = derivative of $Y(\theta)$ with respect to its argument θ
- V_F = volume of fluid reservoir
- V_S = volume of solid body

Greek Letters

α = ratio of volume of fluid to volume of solid
β_n = root of $J_o(\beta_n) = 0$
$\Delta\theta$ = step size in θ for use in numerical solution of integral equation
∇^2 = Laplacian operator
ϵ = fraction of the total volume occupied by solid, defined by Equation (20)
θ = dimensionless time, Dt/L^2
θ^* = generalized dimensionless time, Dt/σ^2
ξ = dummy variable used in integration
σ = ratio of volume of solid body to its external surface
ω = ratio of height to diameter of a cylinder
ω_1, ω_2 = ratios of the two longest sides to the length of the shortest side of a rectangular prism

Subscripts

i = initial
∞ = limiting value as time approaches infinity

LITERATURE CITED

1. Carman, P. C., and R. A. W. Haul, *Proc. Royal Soc.*, **222A**, 109 (1954).
2. Crank, J., "The Mathematics of Diffusion," Oxford at the Clarendon Press, London (1956).
3. ———, *Phil. Mag.*, **39**, 140 (1948).
4. *Ibid.*, 362 (1948).
5. Laudet, M., and H. Oulés, "Symposium on Numerical Treatment of Ordinary Differential Equations, Integral and Integro-Differential Equations, Proceedings of the Rome Symposium," pp. 117-121, Birkhauser-Verlag, Basel (1960).
6. March, H., and W. Weaver, *Phys. Rev.*, **31**, 1072 (1928).
7. Noble, B., "Nonlinear Integral Equations," P. M. Anselone, ed., pp. 215-318, Univ. Wisconsin Press, Madison (1964).
8. Wagner, C., as reported by Zimens, K. E., *Arkiv. Kemi. Min. Geol.*, **20A**, No. 18, 1 (1945).
9. Wilson, A. H., *Phil. Mag.*, **39**, 48 (1948).

Manuscript received September 15, 1967; revision received December 6, 1967; paper accepted January 10, 1968. Paper presented at AIChE St. Louis meeting.

APPENDIX A

The function $f(\theta)$ was obtained by performing the integration indicated in Equation (15) using available (2) solutions for $F(\vec{R}, \theta)$ for each geometry. Derivations for the finite cylinder and rectangular prism were greatly facilitated by use of the Neuman product technique. See Figure 1 for specification of the characteristic length in the definition of θ for each geometry.

Sphere

$$f(\theta) = 1 - \frac{6}{\pi^2}\sum_{n=1}^{\infty}\frac{\exp(-n^2\pi^2\theta)}{n^2} \tag{A1}$$

Infinite cylinder

$$f(\theta) = f_c(\theta) \equiv 1 - 4\sum_{n=1}^{\infty}\frac{\exp(-\beta_n^2\theta)}{\beta_n^2} \tag{A2}$$

with $J_o(\beta_n) = 0$

Infinite slab

$$f(\theta) = f_s(\theta) \equiv 1 - \frac{8}{\pi^2}\sum_{n=0}^{\infty}\frac{\exp[-(2n+1)^2\pi^2\theta/4]}{(2n+1)^2} \tag{A3}$$

Finite cylinder with $\omega \geqq 1$

$$f(\theta) = 1 - [1 - f_c(\theta)][1 - f_s(\theta/\omega^2)] \tag{A4}$$

Finite cylinder with $\omega \leqq 1$

$$f(\theta) = 1 - [1 - f_c(\omega^2\theta)][1 - f_s(\theta)] \tag{A5}$$

Rectangular prism

$$f(\theta) = 1 - [1 - f_s(\theta)][1 - f_s(\theta/\omega_1^2)][1 - f_s(\theta/\omega_2^2)] \tag{A6}$$

APPENDIX B

The numerical method proposed by Laudet and Oulès (5) is very similar to the Runge-Kutta methods commonly used for numerical solution of ordinary differential equations. The pertinent equations used to compute the solutions reported herein are outlined in this appendix. The equation to be solved is:

$$Y(\theta) = G(\theta) - \frac{1}{\alpha}\int_0^\theta Y'(\xi)\,f(\theta - \xi)\,d\xi$$

denote $\theta_n = nh$, $\xi_m = mh$, $f_{m,n} = f(\theta_n - \xi_m)$

$$Y_n = Y(nh),\ Y'_n = Y'(nh),\ G_n = G(nh)$$

To simplify this notation in this appendix only, h is synonymous with the step size $\Delta\theta$.

The following special set of equations is used to calculate $Y_1 = Y(h)$.

Define:

$$\begin{aligned}
k_0 &= G(h) - G(0) - hY'_0 f(h - 0)\\
k_1 &= G(h/3) - G(0) - (1/3)hY'_1 f(h/3 - 0)\\
k_2 &= G(5h/9) - (G(0) - (5/9)hY'_2 f(5h/9 - h/3)\\
k_3 &= G(h) - G(0) - hY'_3 f(h - h/5)\\
k_4 &= G(h) - G(0) - hY'_4 f(h - 9h/10)\\
k_5 &= G(h) - G(0) - hY'_5 f(h - h)
\end{aligned}$$

with:

$$\begin{aligned}
Y'_0 &= (\tilde{Y}_2 - \tilde{Y}_0)/(h/3 - 0)\\
Y'_1 &= (\tilde{Y}_2 - \tilde{Y}_1)/(h/3 - 0)\\
Y'_2 &= (\tilde{Y}_3 - \tilde{Y}_2)/(h/5 - h/2)\\
Y'_3 &= (\tilde{Y}_4 - \tilde{Y}_3)/(9h/10 - h/5)\\
Y'_4 &= (\tilde{Y}_5 - \tilde{Y}_4)/(h - 9h/10)\\
Y'_5 &= (\tilde{Y}_6 - \tilde{Y}_5)/(h - 9h/10)
\end{aligned}$$

and

$$\begin{aligned}
\tilde{Y}_0 &= G(0)\\
\tilde{Y}_1 &= G(0)\\
\tilde{Y}_2 &= G(0) + k_1\\
\tilde{Y}_3 &= G(0) + (24/25)k_1 - (27/125)k_2\\
\tilde{Y}_4 &= G(0) - (837/200)k_1 + 4.131\,k_2\\
\tilde{Y}_5 &= G(0) - (141/16)k_1 + (1269/160)k_2 - (65/224)k_3 - (5/28)k_4\\
\tilde{Y}_6 &= G(0) - (1/18)k_0 + (25/42)k_3 + (50/63)k_4 - 1/3\,k_5
\end{aligned}$$

then

$$Y_1 = Y(h) = \tilde{Y}_6$$

To compute $Y_m = Y(mh)$ for $m > 1$, one of the following equations is used depending upon whether m is even or odd.

$m = 2, 4, 6 \ldots$ (even):

$$\begin{aligned}
Y_m = G_m &- (h/6)(Y'_0 f_{m,0} + 4Y'_1 f_{m,1} + 2Y'_2 f_{m,2} \ldots\\
&+ 4Y'_{m-3} f_{m,m-3} + Y'_{m-2} f_{m,m-2})\\
&- (h/6)(Y'_{m-2} f_{m,m-2} + 4Y'_{m-1} f_{m,m-1} + Y'_m f_{m,m})
\end{aligned}$$

$m = 3, 5, 7 \ldots$ (odd):

$$\begin{aligned}
Y_m = G_m &- (h/6)(Y'_0 f_{m,0} + 4Y'_1 f_{m,1} + \ldots + 4Y'_{m-4} f_{m,m-4}\\
&+ Y'_{m-3} f_{m,m-3}) - (3h/8)(Y'_{m-3} f_{m,m-3} + 3Y'_{m-2} f_{m,m-2}\\
&+ 3Y'_{m-1} f_{m,m-1} + Y'_m f_{m,m})
\end{aligned}$$

The derivatives are approximated as

$$Y'_0 = (Y_1 - Y_0)/h$$

$$Y'_k = (Y_{k+1} - Y_{k-1})/2h \qquad (k = 1 \ldots m-1)$$

Note that $f_{m,m} = f(0) = 0$ and, hence, Y'_m is never required.